Chalcogenide Letters Vol. 8, No. 11, November 2011, p. 659-670

MOLECULAR PHASE SEPARATION EFFECTS ON CALORIMETRIC PROPERTIES OF $Ge_xSe_{80-x}Pb_{20}$ GLASSES

KAMAL KUMAR[a,b*], L. P. PUROHIT [b], R. M. MEHRA [c], AKASH DEEP [d]
[a]*Department of Physics, Government Post Graduate College, Ranikhet 263 647, India*
[b]*Department of Physics, Gurukula Kangri University, Haridwar 249 404, India*
[c]*School of Engineering and Technology, Sharda University, Greater Nodia 201 306, India*
[d]*Biomolecular Electronics and Nanotechnology Division, Central Scientific Instruments Organization, Chandigarh 160 030, India*

The influence of molecular phase separation on thermal activation barriers of phase transformations in $Ge_xSe_{80-x}Pb_{20}$ glasses has been investigated using non-isothermal methods. Kinetic parameters of glass transition, crystallization and decomposition were determined using differential scanning calorimetric and thermo-gravimetric measurements. The model free Kissinger and isoconversional Flynn-Wall-Ozawa methods were employed to calculate the activation energies of thermally induced structural transitions. The observed variation in thermal properties with Ge content in place of Se could be interpreted in terms of the formation of tetrahedrally coordinated Ge-Se structural units at expense of Se-Se units. Deviations in the activation energies of crystallization and decomposition with the extent of conversion indicate the mechanistic complexity of the transformations as these involve different nucleation and growth events due to the presence of different phases. $Ge_xSe_{80-x}Pb_{20}$ glass with $x = 20$ has been found to attain the maximum activation barriers showing high thermal stability and structural rigidity.

(Received October 10, 2011; accepted October 31, 2011)

Keywords: Chalcogenides, Calorimetry, Isoconversional Models, Phase Separation

1. Introduction

Wide optical window (from 1-20 μm), photoinduced reversible structure change and photoinduced anisotropy of germanium based chalcogenides have shown their potentiality in developing advance IR sensors for biomedical process and gas detection [1], optical memories [2] and opto-mechanical actuators [3]. Z-scan measurements of Ge-As-Se glasses [4] have revealed high optical nonlinearity of 24×10^{-18} m^2/W, high refractive index (~2.5) and suitable optical transmission at 1540 nm which make them applicable as core material in optical fibres for telecommunication applications. Studies on local coordination environment of ternary chalcogenides using extended X-ray absorption fine structure (EXAFS) spectroscopy have demonstrated structural homogeneity and chemical order with the microscopic phase separation [5]. Analysis of Ge and As *K*-edge EXAFS spectra of GeAsS/GeAsSe glasses confirms the preservation of chemical order consisting of corner sharing $GeS_4/GeSe_4$ tetrahedra and $AsS_3/AsSe_3$ trigonal pyramids [6].

$Ge_xSe_{80-x}Pb_{20}$ glasses are of particular interest among Ge- chalcogenides due to their p-n transition phenomenon [7]. Radial distribution function obtained by X-ray diffraction on GeSePb glasses [8] have revealed that the Pb is present in Pb^{+2} state and forms iono-covalent bonds with

*Corresponding author: kamalkumar.phy@gmail.com

two non-bridging negatively charged chalcogen atoms which, in turn, form separate covalent bonds with one Ge atom to yield $GeSe_{4/2}$ tetrahedral units. Malik *et al.* [9] performed Electron Paramagnetic Resonance (EPR) spectroscopic measurements on GeSePb system and found no EPR signal because the Pb^{+2} ions do not induce unpaired spins in the system. Therefore, the presence of Pb^{+2} ions does not affect the tetrahedral units of $GeSe_{4/2}$. Using continuous random network model, Tohge *et al.* [7] performed bond concentration calculations on $Ge_xSe_{80-x}Pb_{20}$ glasses, keeping the density of PbSe bonds constant. In the study the above authors inferred that as Ge content increases, the concentration of Ge-Se bonds increases and at 21 at% Ge, the system contains mostly heteropolar Ge-Se bonds in the chemically ordered network stage. This unpins Fermi level and shifts it closer to the conduction band, resulting carrier type reversal at 21 at% Ge [10]. Rabinal *et al.* [11] have carried out calorimetric measurements on $Ge_xSe_{80-x}Pb_{20}$ $(17 \le x \le 24)$ glasses and observed an increase in glass transition temperature T_g and crystallization activation energy E_c up to $x = 21$. Using chemical bond approach, they explained that an increase in the Ge content leads in to a significant cross-linking in the glassy matrix, which raises the cohesive energy and the viscosity of the system thereby resulting an increase in T_g and E_c. Furthermore, two distinct endothermic peaks corresponding to melting were observed and possibility of two microscopic phases was reported. Vaidhyanathan *et al.* [12] studied the coordination environment of GeSePb glasses using infrared, Raman and X-ray absorption near edge spectra (XANES) which illustrated the sp^3d^2 hybridization state of Pb^{+2} to exist in octahedral coordination, whereas Se atoms were in sp^n (n = 1, 2, and 3) hybridization. Lone pairs on Se atoms were polarized towards Pb^{+2} ions suggesting the nature of bonding between Pb and Se to be ionic. Ge enters in tetrahedral coordination utilizing sp^3 state of hybridization for covalent bond formation with Se. The structure of GeSePb glasses was concluded to be iono-covalent, determined by octahedrally coordinated $PbSe_6$ structural units and corner to edge sharing tetrahedral $GeSe_{4/2}$ structural units that were either statistically distributed or interconnected in two matrices.

The above discussion highlights that the structural origin of electrical properties, glass transition and crystallization of $Ge_xSe_{80-x}Pb_{20}$ $(17 \le x \le 24)$ alloys have been widely studied. In a previously published study [13], we investigated for their refractive index profile, dispersion energy and optical bandgap. The results were correlated to suggest the utility of $Ge_xSe_{80-x}Pb_{20}$ glasses in IR optical applications. An extended methodical investigation of phase separation effects on thermal stability enough towards crystallization and decomposition, and chemical durability is further be required for claiming the utility of $Ge_xSe_{80-x}Pb_{20}$ glasses in the preparation and designing of integrated optical components.

In the present report, non-isothermal differential scanning calorimetric (DSC) and thermo-gravimetric (TG) data of $Ge_xSe_{80-x}Pb_{20}$ glasses over the wide region of glass formation $(i.e., x = 0,5,10,15,20,25)$ at different heating rates have been analyzed to examine the kinetics of glass transition, crystallization and thermal decomposition. The activation barriers of thermally induced structure transitions are shown to be essentially dependent on the composition and the extent of conversion. The chemical structure and the thermal properties have been correlated assuming the presence of octahedrally coordinated $PbSe_6$ and tetrahedral $GeSe_{4/2}$ units in the chalcogenide glasses under study.

2. Experimental

$Ge_xSe_{80-x}Pb_{20}$ $(x = 0,5,10,15,20,25)$ glasses were prepared from high purity (5N) Ge, Se and Pb elements (Alfa Aesar) using melt quenching technique. The elements were weighed and sealed in cleaned quartz ampoules under vacuum of 10^{-6} torr. Ampoules were heated to 1000 ºC at a rate of 2 ºC/min in a microprocessor controlled rocking furnace for 18 h and then rocked for 6 h for proper mixing and homogenization of the melt. DSC and TG measurements

were performed with a Perkin Elmer (Pyris™ Diamond) calorimeter. The recording of the temperature and the heat flow for different heating rates were calibrated using the melting temperature of 5N standard of pure zinc and the melting enthalpy of 5N standard of pure indium. The accuracy/precision in the measurements of the temperature and the heat flow were ±0.1 ºC / ±0.01 ºC and < ±1% / < ±0.1%, respectively. For DSC and TG experiments, approximately 20 mg of crushed samples were placed in alumina pans of the calorimeter. The measurements were carried out at heating rates 5, 10, 20 and 50 ºC/min in the temperature range of 0-1000 ºC, in a dynamic atmosphere of nitrogen (200 ml/min). Heat evolved during DSC experiments causes fluctuations in heating rates which perturb kinetic data. As liberation of heat depends on specific heat of the material, the weight of the samples is kept low. The range of heating rates is selected to avoid distortions in the kinetic data due to any possible adverse signal to noise ratio at low temperatures or phase transformations taking place at high temperatures. Dynamic atmosphere of nitrogen eliminates undesired thermal gradients, thus maintaining calibrated conditions of the instrument during the experiments.

For the identification of structural phases formed in amorphous matrix, the initial glassy samples were annealed in a microprocessor controlled furnace (Hindhivac) at the respective peak temperatures of crystallization in a vacuum (~10^{-6} torr) for an hour. The annealed samples were then subjected to X-ray diffraction (XRD) using PANalytical X'pert PRO diffractometer with CuK_{α} radiation.

3. Results

Fig. 1 shows the typical DSC non-isothermograms for $Ge_xSe_{80-x}Pb_{20}$ glasses at a heating rate (β) of 20 ºC/min. The endothermic and exothermic peaks observed in the investigated range of temperature are associated with four phenomena; (i) glass transition which appears as small endothermic peak at temperature T_g, (ii) crystallization related to the exothermic peak at temperature T_{p_c}, (iii) melting indicated by two endothermic peaks at temperatures T_{m_1} and T_{m_2} and (iv) degradation temperature T_{p_d} corresponding to the last endothermic peak. Similar DSC thermograms were obtained at heating rates of 5, 10 and 50 ºC/min. The figure reveals an increase in the values of characteristic temperatures T_g, T_{p_c}, T_{m_1}, T_{m_2} and T_{p_d} upon increasing the Ge concentration from 0 to 20 at%, beyond which the above parameters shift to lower values. Such variations are a consequence of the compositional dependence of thermal properties. The slight increase observed in the enthalpy associated with exothermic peak of crystallization, and endothermic peaks of melting and degradation up to 20 at% Ge is attributed to the increased heat capacity of the system [14].

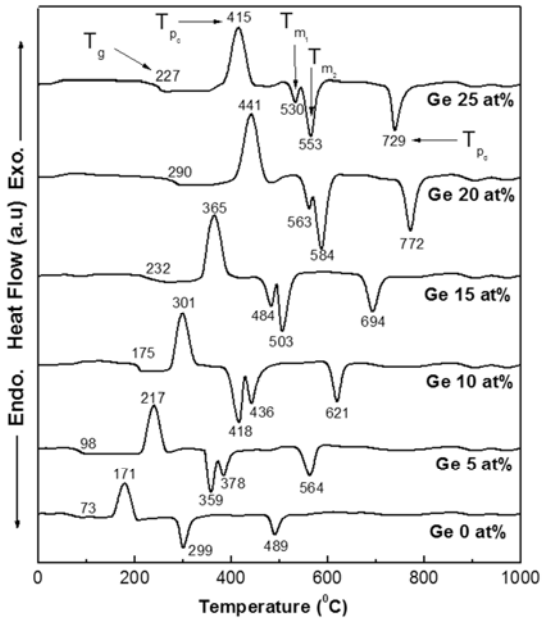

Fig. 1. DSC curves of $Ge_xSe_{80-x}Pb_{20}$ glasses at a heating rate of 20 ºC/min.

T_g represents the strength or rigidity of the glass structure; however, it alone may not account for the thermal stability of glassy state. The stability of a glass towards devitrification can be conveniently estimated by the expression $\Delta T_{cg} = T_{p_c} - T_g$ [15]. Table 1 lists the values of ΔT_{cg} for $Ge_xSe_{80-x}Pb_{20}$ glasses at a scan rate of 20 ºC/min. The values of ΔT_{cg} for all heating scans were found to be maximized at $x = 20$, which reveals the highest thermal stability of the $Ge_{20}Se_{60}Pb_{20}$ glass.

3.1. Kinetics of glass transition

Kinetics of glass transition of amorphous materials is generally described by Lasocka's relationship [16]

$$T_g = A + B \ln \beta \tag{1}$$

where the values of constants A and B depend upon the composition and the method of preparation of the amorphous materials. The physical significance of A and B lie on the effect of heating rates on the structural relaxation within glass transition region. Plots of T_g versus $\ln \beta$ and linear fitting of data points, as shown in Fig. 2, illustrate the validity of Eq. (1) for $Ge_xSe_{80-x}Pb_{20}$ glasses. The values of A and B (Table 1) range between 18.90-168.93(±2) ºC and 17.88-39.59(±1) min, respectively with maximums observed for 20 at% Ge.

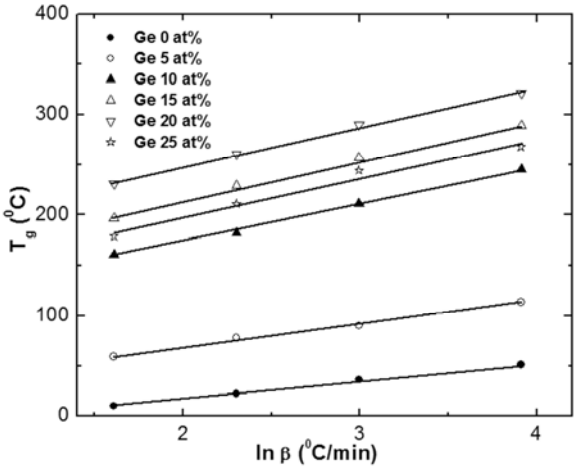

Fig. 2. Lasocka plot for glass transitions of $Ge_xSe_{80-x}Pb_{20}$ glasses

A number of reports [17-19] based on the structural relaxation model has explained the dependence of heating and cooling rates on the glass transition temperature. Kissinger's model free method [20] for reaction order models based on the given Eq. (2) is more commonly used to calculate activation energy (E_a) of transition.

$$\frac{d\alpha}{dt} = A\exp\left(\frac{-E_a}{RT}\right) f(\alpha) \tag{2}$$

where α is the extent of reaction, t the time, T the temperature, A the pre-exponential factor, R the molar gas constant and $f(\alpha) = (1-\alpha)^n$ is the reaction model which explicates the dependence of conversion rate on the extent of reaction with n being the empirical order of reaction. In non-isothermal process, the temperature T is raised with a constant heating rate $\beta = \frac{dT}{dt}$. In Kissinger model, the maximum reaction rate occurs when $\frac{d^2\alpha}{dT^2} = 0$, from which the following equation is obtained

$$\frac{E_a\beta}{RT_m^2} = A\left\{n(1-\alpha)_m^{n-1}\right\}\exp\left(\frac{-E_a}{RT_m}\right) \tag{3}$$

where T_m is the temperature at which the peak (i.e. inflection point) of differential thermal analysis (or DSC) deflection occurs. Natural logarithm of Eq. (3) and rearranging gives

$$\ln\left(\frac{\beta}{T_m^2}\right) = \ln\left[\frac{AR\left\{n(1-\alpha)_m^{\,n-1}\right\}}{E_a}\right] - \frac{E_a}{RT_m} \tag{4}$$

E_a can be calculated by Arrhenius plotting of $\ln\left(\frac{\beta}{T_m^2}\right)$ versus $\frac{1}{T_m}$. The activation energies of glass transition (ε_g) for $Ge_xSe_{80-x}Pb_{20}$ samples deduced from the slope of $\ln\left(\frac{\beta}{T_g^2}\right)$ versus $\frac{1}{T_g}$ plots (shown in Fig. 3) are listed in Table 1. The increase in ε_g (from 155.26 to 233.33(±3)

kJ/mol) observed with increasing Ge content (from 0 to 20 at%) indicates the formation of a stressed rigid structure.

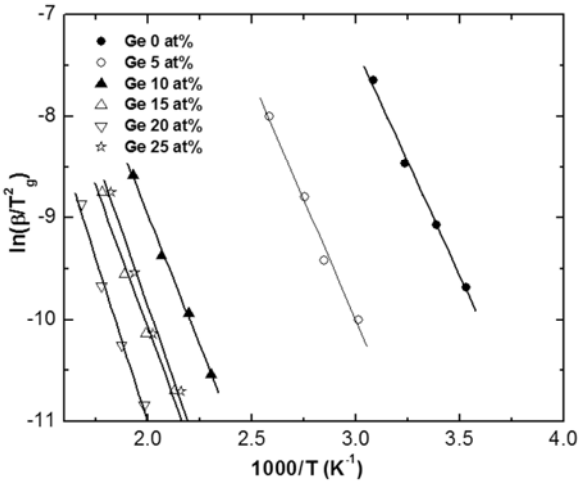

Fig. 3. Kissinger plot for glass transitions of $Ge_xSe_{80-x}Pb_{20}$ glasses

3.2. Kinetics of crystallization

Nucleation and growth are two individual processes governing the crystallization of glasses. In non-isothermal conditions, the initials stage of crystallization leads to the nucleation. The crystallization exotherm then illustrates the growth of crystalline phase. Nucleation-growth model for isothermal transformations, postulated by Johnson-Mehl-Avrami (JMA) [21-23] has been used frequently for the analysis of non-isothermal kinetic data also [24]. The model basically works on an assumption that the nucleation takes place very rapidly and at once [25] implying a single step crystallization process, but in practice, the validity of this theory is difficult to be authenticated [26]. In the present study, the Kissinger's model free method (Eq. (4)) has been preferred for estimating the activation energies of crystallization (E_c) of $Ge_xSe_{80-x}Pb_{20}$ glasses. Slopes of linear fits of $\ln\left(\frac{\beta}{T_{p_c}^2}\right)$ versus $\frac{1}{T_{p_c}}$ plots (Fig. 4) determine E_c as listed in Table 1. The increasing value [91.33-114.99(±3) kJ/mol] of E_c with increasing concentration of Ge up to 20 at% testifies that the substitution of Se for Ge enhances the thermal stability of the studied glasses.

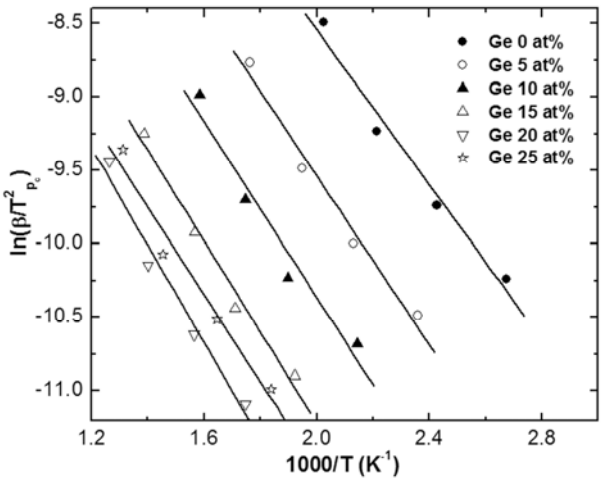

Fig. 4. Kissinger plot for crystallization of $Ge_xSe_{80-x}Pb_{20}$ glasses

Crystallization and decomposition of chalcogenide glasses can be either single step or complex depending on the composition and the method of preparation [27]. The model free Flynn-Wall-Ozawa's (FWO) isoconversional method [28, 29] based on the evaluation of kinetic parameters at progressive conversion values has been applied successfully to study single step or complex reaction mechanisms of crystallization and decomposition [30, 31]. FWO isoconversional rate law defined as Eq. (6) is derived by employing Doyle approximation [32] to the Arrhenius integral in Eq. (5), which, in turn, is an integral form of the non-isothermal kinetic Eq. (2)

$$\int_0^{\alpha} \frac{1}{(1-\alpha)^n} d\alpha = \frac{A}{\beta} \int_0^{T} \exp\left(-\frac{E_a}{RT}\right) dT \tag{5}$$

$$\ln \beta = \ln \frac{AE_a}{g(\alpha)R} - 2.315 - 0.457 \frac{E_a}{RT} \tag{6}$$

A slope of $\ln \beta$ versus $\frac{1}{T}$ plot yields the activation energy of crystallization (E_{c_α}) of a particular fraction α_c crystallized at a specific temperature T. The estimation of α_c can be carried out as $\alpha_c = \frac{\Delta H_{\alpha_c}}{\Delta H}$. ΔH and ΔH_{α_c} represent the total heat released during the crystallization and the heat released at a given α_c, respectively. The former parameter is determined by correlation with the total area of DSC exotherm, while the latter parameter is determined by calculating the area of DSC exotherm between the starting temperature of crystallization and temperature corresponding to α_c. Fig. 5 shows the variation in the values of E_{c_α} as a function of α_c for the $Ge_xSe_{80-x}Pb_{20}$ glasses. The values of E_{c_α} are observed within a range of 90-123(±2) kJ/mol exhibiting maximum activation barrier against conversion for $x = 20$. This observation reconfirms that the glass with the composition $Ge_{20}Se_{80}Pb_{20}$ has highest thermal stability. It is also observed that for the composition corresponding to $x = 0$, the values of E_{c_α} are independent of the degree of conversion α_c. This directly suggests a single step conversion process. For all other compositions of $Ge_xSe_{80-x}Pb_{20}$ glasses, the values of E_{c_α} follow a slightly upward trend with a positive change in α_c, which reveal the involvement of multiphase reaction kinetics due to the presence of different phases [33]. This excludes the applicability of JMA model to the experimental data of $Ge_xSe_{80-x}Pb_{20}$ glasses, with the exception of the composition corresponding to $x = 0$. Similar observations were reported for SeTeSb glasses where the total transformation reaction involved simultaneous different nucleation and growth processes [34, 35].

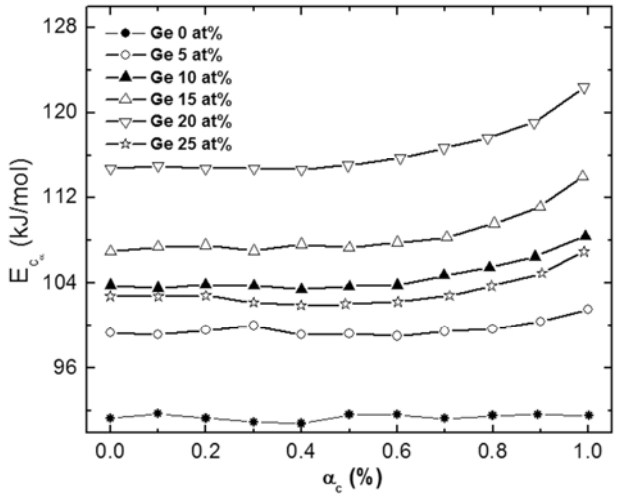

Fig. 5. Variation of activation energies of crystallization E_{c_α} *as a function of crystallized fraction* α_c

3.3. Kinetics of decomposition

Fig. 6 represents the TG or weight loss curves for $Ge_xSe_{80-x}Pb_{20}$ glasses in the temperature range of investigation at a heating rate of 20 ºC/min. The curves depict that the glassy samples preserve thermal stability till their melting. Similar weight loss behaviour has been obtained at heating rates of 5, 10 and 50 ºC/min. It is observed that the composition corresponding to $x = 20$ has minimum rate of weight loss. The activation energies of thermal decomposition (E_{t_d}) as a function of conversion α_d (defined as the % weight loss at any temperature) have been computed from slopes of $\ln\beta$ versus $\frac{1}{T}$ plots by means of FWO isoconversional rate law Eq. (6). Fig. 7 illustrates the variation in the values of E_{t_d} with α_d for various Ge contents. The slight increase observed in E_{t_d} of Ge containing glasses with changing α_d exemplifies complex decomposition kinetics. The values of E_{t_d} at $\alpha_d = 50\%$ are listed in Table 1. The increase in E_{t_d} from 105.14 to 142.18(±2) kJ/mol with increasing Ge concentration from 0 to 20 at% can be ascribed to the formation of new phase into PbSe matrix. However, the decrease observed in E_{t_d} for the sample with 25 at% of Ge indicates the reduction in mean bond energy of the system.

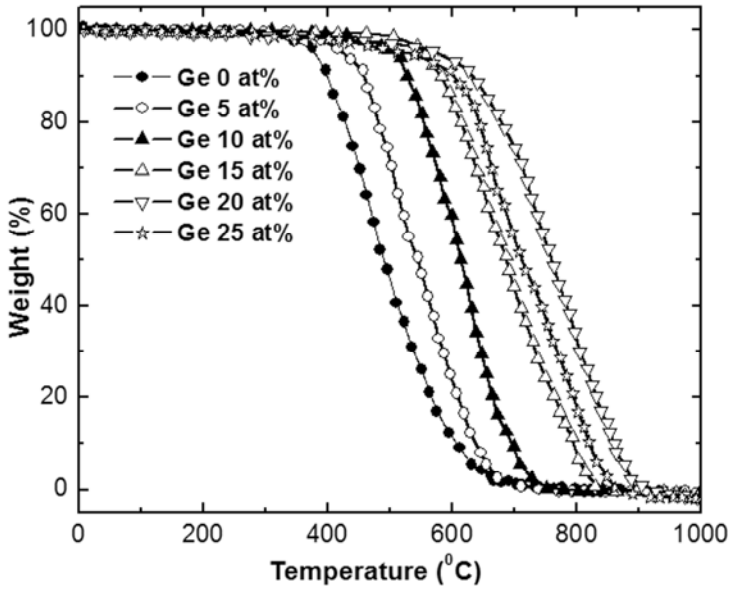

Fig. 6. TG curves of $Ge_xSe_{80-x}Pb_{20}$ glasses at a heating rate of 20 ºC/min.

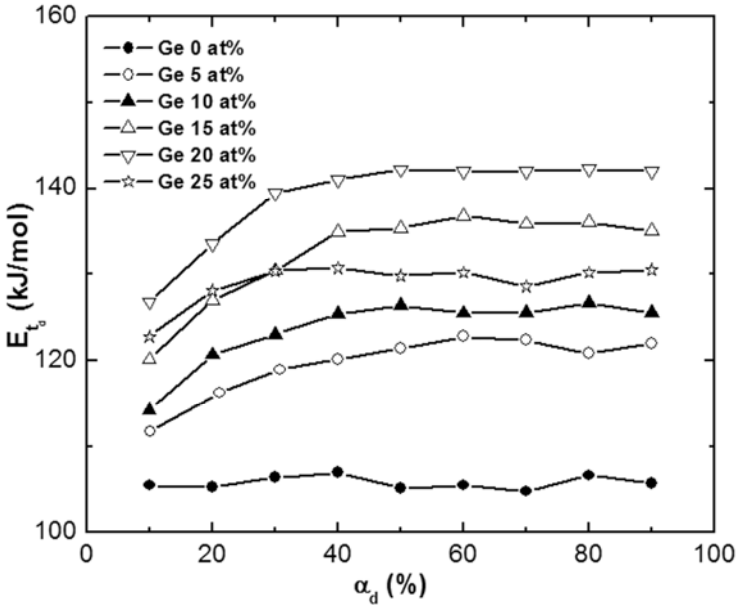

Fig. 7. Variation of activation energies of decomposition E_{t_d} as a function of decomposed fraction α_d

3.4. XRD Analysis

Fig. 8 depicts the XRD patterns of $Ge_xSe_{80-x}Pb_{20}$ glasses annealed at their respective peak crystallization temperatures which were obtained at heating rate of 20 ºC/min. The intensity peaks identified as (020), (100), (200) and (311) belonging to $GeSe_{4/2}$, Se-Se, $PbSe_6$ and Ge-Ge units, respectively, confirm the presence of multiphase state in the studied glasses. It is observed that the peak intensity corresponding to (020) plane increases while that for (100) plane decreases with increasing Ge concentration up to 20 at%. This reveals the creation of $GeSe_{4/2}$ phase into $PbSe_6$ matrix. In case of $x = 20$ composition, the (020) and (200) planes prevail over all other planes. The observed steadiness in peak intensity of $PbSe_6$ units indicates that the density of PbSe bonds remains invariable. However, for the sample with 25 at% of Ge, the appearance of (311) planes in the diffraction pattern exhibits the presence of Ge-Ge bonds.

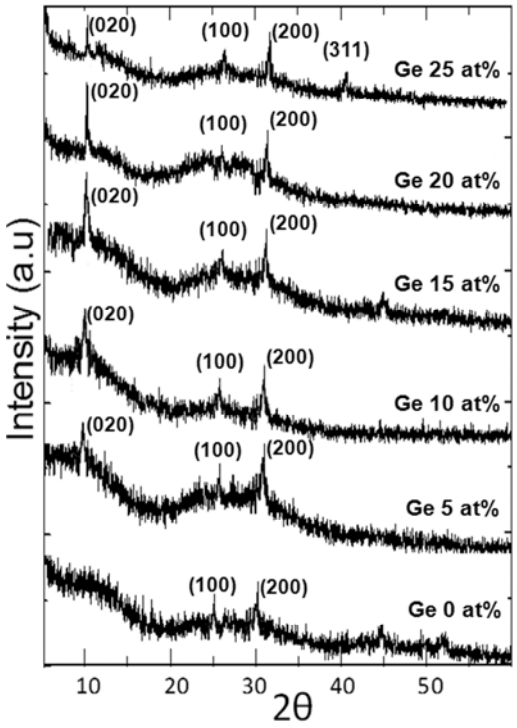

Fig. 8. X-ray diffractograms of $Ge_xSe_{80-x}Pb_{20}$ glasses at different Ge content.

Table 1. Characteristic temperatures and activation energies of glass transition, crystallization and degradation of $Ge_xSe_{80-x}Pb_{20}$ glasses

Ge content at%	ΔT_{cg}	Lasocka parameters		ε_g kJ/mol	E_c kJ/mol	E_{t_d} at 50% conversion kJ/mol (±2)
		A °C	B min			
0	98	18.9	17.98	155.26	91.33	105.14
5	119	22.12	23.33	164.98	99.35	121.56
10	126	99.62	32.01	177.81	103.83	126.31
15	133	135.28	37.82	192.07	107.72	135.12
20	151	168.93	39.59	223.33	114.99	142.18
25	138	140.01	36.07	203.52	102.78	129.67

4. Discussion

The activation energies of glass transition, crystallization and thermal decomposition obtained by model free and isoconversional methods are substantially increased upon the introduction of Ge into PbSe matrix and become maximized at Ge = 20 at%. The incorporation of Ge atoms leads to the percolation of $GeSe_{4/2}$ units into the $PbSe_6$ matrix. The whole process is accompanied by a decrease in the number of unsaturated Se-Se bonds and a simultaneous increase in the number of saturated Ge-Se bonds, as bond energies decrease in the order of Ge-Se (206.49 $kJmol^{-1}$) to Se-Se (183.92 $kJmol^{-1}$) [12]. Ultraviolet and X-ray photoemission studies [36] testify that heteropolar Ge-Se bonding is preferred over like-atom bonds (Se-Se or Ge-Ge) to retain fourfold and twofold coordination of germanium and selenium, respectively. At 20 at% Ge, the

system contains mainly Ge-Se bonds with Pb-Se bonds as illustrated in XRD reflections (Fig. 8) and Raman experiments [12]. This results in to the formation of highly connected and continuous regions. Therefore, $Ge_{20}Se_{60}Pb_{20}$ glass exhibits large activation barriers for phase transformations. However, at Ge = 25 at%, homopolar Ge-Ge (157.16 $kJmol^{-1}$) bonds become predominant in addition to Ge-Se bonds. The presence of Ge-Ge bonds reduces mean bond energy of the system causing a lowering in the values of related thermal parameters.

The observed variations in E_{c_α} with α_c (Fig. 5) signify that the $PbSe_6$ and $GeSe_{4/2}$ units in $Ge_xSe_{80-x}Pb_{20}$ glasses undergo different mechanism of nucleation and growth. Due to higher bond energy, crystallization of $GeSe_{4/2}$ unit legs behind that of $PbSe_6$ unit thereby initiating at relatively elevated temperatures. This feature maximizes at Ge = 20 at% due to maximum concentration of Ge-Se bonds. Two endothermic peaks (Fig. 1) associated with the melting of GeSePb glasses suggest the occurrence of phase separation in the system. The temperatures T_{m_1} and T_{m_2} can be assigned to the successive melting of $PbSe_6$ and $GeSe_{4/2}$ phases, respectively. The fluid from the melting of $PbSe_6$ units would react with the remaining units to yield final melting at the liquidus. Fig. 6 shows one step weight loss indicating that the overall decomposition takes place in a single step. This confirms the interconnectivity of structural units. The highest values of T_{p_d} and E_{t_d} observed for $Ge_{20}Se_{60}Pb_{20}$ glass proves its better thermal durability than other compositions of $Ge_xSe_{80-x}Pb_{20}$ glasses.

5. Conclusion

Non-isothermal phase transformation kinetics of $Ge_xSe_{80-x}Pb_{20}$ $(x = 0,5,10,15,20,25)$ glasses has been investigated using Lasocka method, Kissinger's model free method and Flynn-Wall-Ozawa's isoconversional method. The study demonstrates the phase separations at a molecular level and hindrance of weight loss during phase transitions. The ternary composition $Ge_{20}Se_{60}Pb_{20}$ exhibited the thermal stability against devitrification as it attains highest activation energy of glass transition and crystallization. This composition also reveals an increased enthalpy which indicates formation of the stressed rigid structure. Highest interconnectivity between $PbSe_6$ and $GeSe_{4/2}$ units for $Ge_{20}Se_{60}Pb_{20}$ glass is ascertained with the highest activation barrier for decomposition. Therefore, it infers from the thermal analysis that the high thermal stability and structural rigidity of $Ge_{20}Se_{60}Pb_{20}$ glass make it a strong contender for optical fibres and waveguide applications in IR optics.

Acknowledgments

One of the authors (Kamal Kumar) acknowledges CSIR, India for providing financial assistance in the form of Senior Research Fellowship (SRF). Thanks are also due to Institute Instrumentation Centre, IIT Roorkee, India for DSC and TG measurements.

References

[1] A. A. Wilhelm, C. Boussard-Plédel, Q. Coulombier, J. Lucas, B. Bureau, P. Lucas, Adv. Mater. **19,** 3796 (2007).
[2] A. V. Kolobov, P. Fons, A. I. Frenkel, A. L. Ankudinov, J. Tominaga, T. Uruga, Nat. Mater. **3,** 703 (2004).
[3] P. Krecmer, A. M. Moulin, R. J. Stephenson, T. Rayment, M. E. Welland, S. R. Elliott, Science **277,** 1799 (1997).
[4] J. T. Gopinath, M. Soljacic, E. P. Ippen, V. N. Fuflyigin, W. A. King, M. Shurgalin, J. Appl. Phys. **96**, 6931 (2004).
[5] A. Ganjoo, H. Jain, S. Khalid, C. G. Pantano, Phil. Mag. Lett. **85**, 503 (2005).
[6] S. Sen, B. G. Aitken, Phys. Rev. B **66**, 134204 (2002).
[7] N. Tohge, H. Matsuo, T. Minami, J. Non-Cryst. Solids **95**, 809 (1987).

[8] S. C. Rowland, F. Ritland, D. H. Burns, A. Bienenstock, Proc. of the 7th Int. Conf. on Amorphous and Liquid Semiconductors (Edinburgh Bristol: Institute of Physics), 135 (1977).
[9] S. K. Malik, K. L. Bhatia, N. Kishore, J. S. Phor, J. Non-Cryst. Solids **142**, 55 (1992).
[10] K. L. Bhatia, S. K. Malik, N. Kishore, S. P. Sing, Phil. Mag. B **66**, 587 (1992).
[11] M. K. Rabinal, N. R. Rao, K. S. Sangunni, E. S. R. Gopal, Phil. Mag. B **70**, 89 (1994).
[12] B. Vaidhyanathan, S. Murugavel, S. Asokan, K. J. Rao, J. Phys. Chem. B **101** 9717 (1997).
[13] Kamal Kumar, L. P. Purohit, R. Kumar, R. M. Mehra, J. Phys. D: Appl. Phys. **42**, 115108 (2009).
[14] R. Rajesh, J. Philip, J. Appl. Phys. **93**, 9737 (2003).
[15] A. Dietzel, Glasstech. Ber. **22**, 1187 (1968).
[16] M. Lasocka, Mater. Sci. Eng. **23,** 173 (1976).
[17] C. T. Moynihan, A. J. Easteal, J. Wilder, J. Phys. Chem. **78**, 2673 (1974).
[18] Y. Yue, R. V. Ohe, S. L. Jensen, J. Chem. Phys. **120**, 8053 (2004).
[19] I. Avramov, N. Avramova, J. Non-Cryst. Solids **260**, 15 (1999).
[20] H. E. Kissinger, Anal. Chem. **29,** 1702 (1957).
[21] W. A. Johnson, R. F. Mehl, Trans. Am. Inst. Min. Met. Eng. **135,** 416 (1939).
[22] M. Avrami, J. Chem. Phys. **8**, 212 (1940).
[23] M. Avrami, J. Chem. Phys. **9**, 177 (1941).
[24] K. Matusita, T. Konatsu, R. Yokota, J. Mater. Sci. **19**, 291 (1984).
[25] J. Malek, D. Svadlak, T. Mitsuhashi, H. Haneda, J. Non-Cryst. Solids **352**, 2243 (2006).
[26] K. Chrissafis, T. Kyratsi, K.M. Paraskevopoulos, M.G. Kanatzidis, Chem. Mater. **16,** 1932 (2004).
[27] J. Malek, Thermochim Acta **355**, 239 (2000).
[28] J. H. Flynn, L. A. Wall, Polym. Lett. **4**, 323 (1966).
[29] T. Ozawa, J. Therm. Anal. **2**, 301 (1970).
[30] K. Chrissafis, T. Kyratsi, K. M. Paraskevopoulos, M. G. Kanatzidis, Chem. Mater. **16,** 1932 (2004).
[31] S. Vyazovkin, W. Linert, J. Solid. State Chem. **114**, 392 (1995).
[32] C. D. Doyle, Nature **207**, 290 (1965).
[33] A. Khawam, Douglas R. Flanagan, Thermochim. Acta **436**, 101 (2005).
[34] A. A. Joraid, Thermochim. Acta **436**, 78 (2005).
[35] A. A. Abu-Sehly, Thermochim. Acta **485**, 14 (2009).
[36] K. Inoue, T. Katayama, K. Kawamoto, K. Murase, Phys. Rev. B **35,** 7496 (1987).